SODIUM ZINC CARBONATE AS PRECURSOR OF NANO-ZnO IN PHOTOACTIVE NANOCOMPOSITES PREPARED BY CALCINATION PROCESS

TOKARSKÝ Jonáš[1,2], JANÍKOVÁ Barbora[3], MAMULOVÁ KUTLÁKOVÁ Kateřina[1], CHLEBÍKOVÁ Lucie[1]

[1]*Nanotechnology Centre, VSB - Technical University of Ostrava, Czech Republic, EU*

[2] *IT4Innovations, VSB - Technical University of Ostrava, Czech Republic, EU*

[3]*Faculty of Metallurgy and Materials Engineering, VSB - Technical University of Ostrava, Czech Republic, EU*

Abstract

Kaolin/ZnO nanocomposites were prepared by heat-induced (100 - 600 °C) decomposition of sodium zinc carbonate clusters synthesized from zinc chloride and sodium carbonate in water suspension of kaolinite-rich kaolin KKAF. X-ray diffraction analysis revealed that highly crystalline ZnO nanoparticles (NPs) are obtained in nanocomposite at a temperature above 400 °C. According to X-ray fluorescence spectroscopy, nanocomposites contain ~ 40 wt.% of ZnO NPs. Ultrafine ZnO NPs evenly distributed on the kaolinite surface were observed using transmission electron microscopy. Preferred growth of ZnO NPs on different kaolinite surfaces was investigated using molecular simulations. All nanocomposites (and pristine ZnO NPs prepared similarly as control samples) were characterized also by UV-VIS diffuse reflectance spectroscopy. Photocatalytic activity (tested by discoloration of Acid Orange 7 aqueous solution) of the nanocomposites was found higher than of pristine ZnO NPs which together with high stability (according to leaching tests) is a good prerequisite for the use of samples in various green applications.

Keywords: Sodium zinc carbonate, nano-ZnO, phyllosilicate, calcination, photoactivity

1. INTRODUCTION

Zinc oxide nanoparticles (ZnO NPs) are intensively studied due to photocatalytic properties (E_g = 3.37 eV) and variety of resulting practical applications, especially in the field of cleaning the environmental pollution [1,2]. Although the band gap energy of another well-known photocatalyst TiO_2 is slightly lower (E_g = 3.20 eV), i.e., not so short wavelength is necessary to the initiation of catalytic effect, the ZnO is considered to be less expensive in comparison with TiO_2 [2]. Moreover, Hayat et al. [3] reported higher photocatalytic activity of ZnO in comparison with classical reference material P25 TiO_2 Degussa. Various precursors usable for synthesis of ZnO NPs were reported ($Zn(NO_3)_2$ [3], $ZnCl_2$ [4], etc.), however, quite little attention has been paid to the sodium zinc carbonate ($Na_2Zn_3(CO_3)_4 \cdot 3H_2O$) which can be synthesized e.g. from $NaHCO_3$ in $ZnCl_2$ solution [5]. The current practical use of $Na_2Zn_3(CO_3)_4 \cdot 3H_2O$ includes Zn(II) supplementation [5] or inhibition of zinc corrosion [6]. Since the possible danger to the environment and human health from freely spreaded photoactive NPs is still the subject of a lively discussion [7,8], it is reasonable to prevent the spread by anchoring the NPs on at least microsized solid crystalline substrate. Phyllosilicates as suitable substrates for photocatalytic NPs were widely discussed by Matějka and Tokarský [9]. Although the phyllosilicates of 2:1 type are often used for this purpose [9], the phyllosilicate of 1:1 type, kaolinite, was also revealed as efficient substrate [9,10]. It is not only because of its abundance and low price but also because of its pozzolanic activity [11,12].

Aims of experiments in this study were to prepare the photoactive kaolin/ZnO nanocomposite using $Na_2Zn_3(CO_3)_4 \cdot 3H_2O$ as precursor, to thoroughly characterize structure of the nanocomposite, to evaluate photocatalytic properties and stability of the nanocomposite.

2. MATERIALS AND METHODS

2.1. Preparation of the samples

Size fraction < 80 μm was prepared from kaolin KKAF (LB Minerals). Chemical compounds Na_2CO_3 p.a., $ZnCl_2$ p.a. (Lach-Ner), and Acid orange 7 (Synthesia) were used as received. Mixing the kaolin KKAF (denoted as K) with $ZnCl_2$ in Na_2CO_3 saturated aqueous solution led to the formation of kaolin/$Na_2Zn_3(CO_3)_4 \cdot 3H_2O$ precursor which was after filtration and drying at 100 °C calcined for 1 h at 400, 500, and 600 °C. Such obtained nanocomposites were denoted as K-ZnO(T) where T represents the temperature used, i.e., 100, 400, 500, 600 °C. Pristine ZnO NPs were prepared similarly without presence of K and were denoted as ZnO(T) where T has the same meaning as in the previous case.

2.2. Characterization methods

Samples were studied by energy dispersive fluorescence spectroscopy (XRFS) using SPECTRO XEPOS (SPECTRO Analytical Instruments GmbH) equipped with 50 W Pd X-ray tube, X-ray powder diffraction analysis (XRPD) using $Co_{K\alpha}$ irradiation (λ = 1.789 nm) in Bruker D8 Advance diffractometer (Bruker AXS), transmission electron microscopy (TEM) using JEOL 2010 HC (JEOL Ltd.) with accelerating voltage 160 kV, UV-VIS diffuse reflectance spectroscopy (UV-VIS DRS) using CINTRA 303 (GBC Scientific Equipment), and molecular modeling using Universal force field [13] in the Materials Studio/Forcite module (Biovia). Photoactivity of the samples was evaluated by discoloration of Acid orange 7 (AO7) aqueous solution (c_0 = $3.5 \cdot 10^{-4}$ mol·dm^{-3}). Sample (m = 0.05 g) in 0.1 dm^3 of the solution was stirred for 24 h to achieve adsorption equilibrium and after 24 h the dispersion was exposed to UV irradiation (λ = 368 nm) for 1 h. Absorbance of AO7 aqueous solution obtained by filtration was measured using Fiber optic spectrometer USB4000 (OceanOptics, USA) at 480 nm. Stability of the nanocomposites, i.e., release of Zn from the nanoparticles anchored on K matrix, was evaluated using leaching test according to the European technical standard EN 12457-2. Sample (m = 1 g) was shaken for 24 h in 0.01 dm^3 of distilled water, the liquid portion was separated using filtration and amount of Zn in extract was determined using emission spectrometer with inductively coupled plasma (Spectro Ciros Vision).

3. RESULTS AND DISCUSSION

Chemical composition of K, K-ZnO(100), and K-ZnO(400) samples obtained by XRFS is shown in **Table 1**. In the case of dried nanocomposite K-ZnO(100), the formation of zinc-containing phases can be seen, and further increase in ZnO content after calcination at 600 °C is evident. Much higher loss on ignition (LOI) for K-ZnO(100) in comparison with K-ZnO(600) can be explained by decomposition of the zinc-containing phases during the calcination.

Table 1 Composition of kaolin and K-ZnO nanocomposites dried at 100°C and calcined at 600 °C. LOI - loss on ignition

	Al_2O_3 (wt.%)	SiO_2 (wt.%)	ZnO (wt.%)	LOI (wt.%)
K	34.80	49.70	0.00	11.52
K-ZnO(100)	18.96	24.13	33.21	21.00
K-ZnO(600)	24.69	32.06	38.70	1.36

XRPD patterns of all samples are summarized in **Figure 1**. Preparation process described in section *2.1.* led to the formation of $Na_2Zn_3(CO_3)_4 \cdot 3H_2O$ (PDF no. 01-0457) but also other products, $Zn_4CO_3(OH)_6 \cdot H_2O$ (PDF no. 00-011-0287), $Zn_5(CO_3)_2(OH)_6$ (PDF no. 00-024-0256), and NaCl (PDF no. 00-001-0994), were detected in diffraction pattern of ZnO(100) sample (**Figure 1a**). During calcination, the compounds were decomposed and gave rise to the ZnO (wurtzite structure, PDF number 70-2551), whose crystallinity increased with

increasing calcination temperature. Sharp and narrow reflections indicating full crystallinity can be found in XRPD pattern of ZnO(600) sample (**Figure 1a**). XRPD pattern of K sample (**Figure 1b**) shows kaolinite (PDF no. 58-2005) as a dominant phase accompanied by muscovite (PDF no. 58-2034) and quartz (PDF no. 46-1045). In dried nanocomposite K-ZnO(100) the $Na_2Zn_3(CO_3)_4 \cdot 3H_2O$ was formed, and - similarly to the previous case - the ZnO (hexagonal, PDF number 70-2551) was formed and its crystallinity increased during the calcination (**Figure 1b**). Disappearance of kaolinite basal reflection observable in K-ZnO(600) diffraction pattern is the consequence of kaolinite → metakaolinite phase transformation [12].

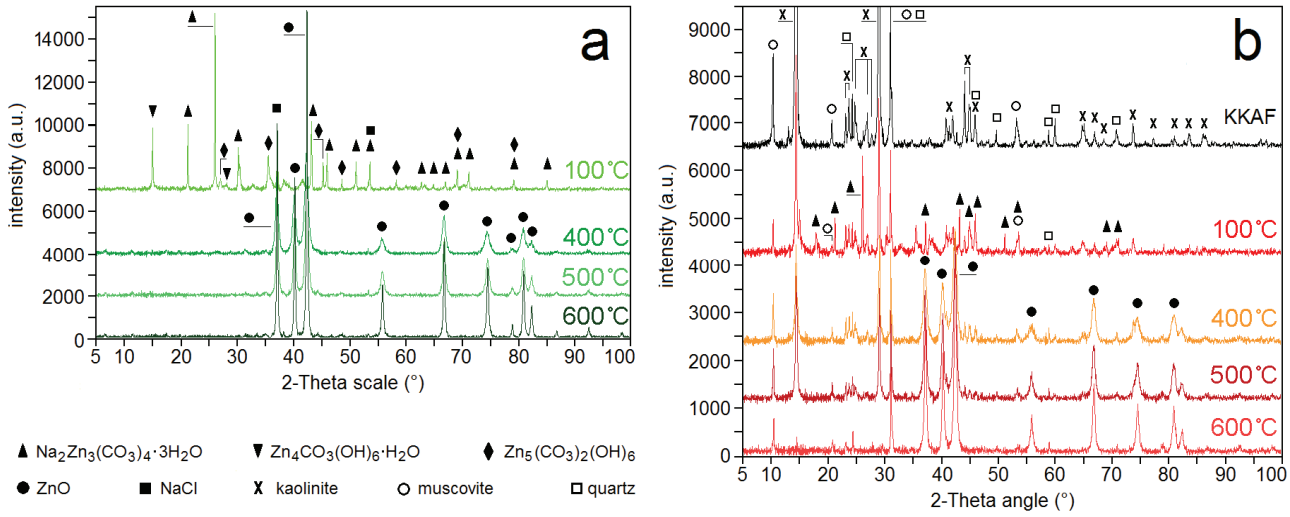

Figure 1 XRPD patterns of (a) pure ZnO NPs and (b) pure kaolin KKAF and K-ZnO nanocomposites

ZnO(*1 0 1*) reflections (2θ = 42.36°) were used to calculate crystallite sizes (L_c) of ZnO for all samples according to Scherrer formula [14]. Lanthanum hexaboride was used as standard and L_c values are listed in **Table 2**. Both for pure NPs and nanocomposites the increase of L_c in dependence on temperature is evident. Up to 500 °C the sizes are very similar, however, significant difference occurs at 600 °C when L_c for K-ZnO(600) is two-fifths lower than L_c for ZnO(600). **Table 2** also shows band gap energies E_g (calculated from UV-VIS reflectance spectra) and corresponding wavelengths (λ). Only negligible increase in E_g (~ 0.6 %) was observed for ZnO NPs in nanocomposites in comparison with pure ZnO NPs.

Table 2 Crystallite sizes (L_c), band gap energies (E_g), and corresponding wavelengths (λ) for ZnO NPs and K-ZnO nanocomposites calcined at 400 - 600 °C

	ZnO(400)	ZnO(500)	ZnO(600)	K-ZnO(400)	K-ZnO(500)	K-ZnO(600)
L_c (nm)	16	24	44	14	21	27
E_g (eV)	3.29	3.29	3.29	3.31	3.31	3.31
λ (nm)	376.83	376.83	376.54	374.94	374.48	374.48

TEM images of ZnO(600) NPs and K-ZnO(600) nanocomposite are compared in **Figure 2**. Difference in size of ZnO NPs in both samples is evident and since size of the most ZnO NPs in the nanocomposite is smaller than L_c value (27 nm; see **Table 2**), the most NPs can be considered monocrystalline. Moreover, uniform distribution of ZnO NPs on the kaolinite was found (also for K-ZnO(400) and K-ZnO(500); images not shown) and the ZnO NPs were observed both on the surface and on the edges of kaolinite.

Crystallographic orientation of ZnO NPs on three different kaolinite surfaces - tetrahedral (T), octahedral (O), edge - was studied using molecular modeling. Kaolinite was prepared as nonperiodic superstructure $Al_{1254}Si_{1296}O_{3156}(OH)_{2640}$ containing six layers.

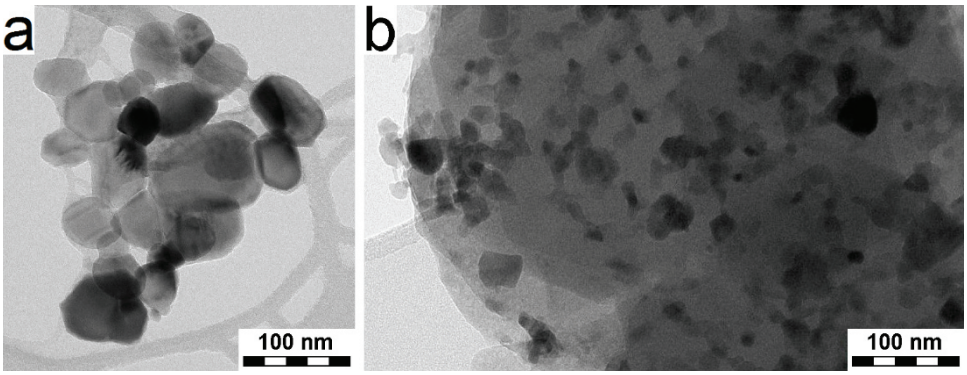

Figure 2 TEM images of (a) pure ZnO(600) nanoparticles and (b) K-ZnO(600) nanocomposite

Total charge −6 el. arising from the non-stoichiometry on the edges was compensated by ZnO NP ($Zn_{186}O_{183}$) adjacent to one of the three surfaces of kaolinite. Four ZnO NPs with different orientation, *(0 0 1)*, *(1 0 0)*, *(1 1 0)*, *(1 0 1)*, but with the same number of atoms (20 Zn) in the *(h k l)* plane directly adjacent to the kaolinite, were prepared and placed on each of the three surfaces. Four *(h k l)* planes on three surfaces gives twelve initial models but since five various positions of each ZnO NP on given surface were tested, sixty initial models were prepared in total. After geometry optimization, models with the lowest total potential energies were selected and interaction energies E_{int} per interface area (20 Zn atoms in different *(h k l)* planes leads to different sizes of interface areas) were calculated according to the formula $E_{int} = E_{TP,M} - (E_{TP,ZnO} + E_{TP,K}) / S$, where $E_{TP,M}$ ($kJ \cdot mol^{-1}$) is total potential energy of whole model, $E_{TP,ZnO}$ ($kJ \cdot mol^{-1}$) is E_{TP} of ZnO NP, $E_{TP,K}$ ($kJ \cdot mol^{-1}$) is E_{TP} of kaolinite, and S ($Å^2$) is the interface area, i.e. area of ZnO NP adjacent to the kaolinite. Results are summarized in **Table 3** where interface areas are also listed.

Table 3 Interaction energies E_{int} ($kJ \cdot mol^{-1} \cdot Å^{-2}$) for each ZnO NP adjacent via given *(h k l)* plane to one of three different surfaces of kaolinite. Interface areas S ($Å^2$) for each *(h k l)* plane of ZnO NP are also provided

(hkl) plane of ZnO NP	*(1 0 1)*	*(1 0 0)*	*(0 0 1)*	*(1 1 0)*
S	108	203	147	233
E_{int} (ZnO on T surface of kaolinite)	-336	-206	-154	-109
E_{int} (ZnO on O surface of kaolinite)	-253	-190	-150	-100
E_{int} (ZnO on edge of kaolinite)	-173	-154	-114	-116

Negative E_{int} values (the lower the E_{int}, the stronger the interaction) reveal that ZnO NPs can grow on each type of kaolinite surfaces. This result corresponds with full coverage observed by TEM. Sequence of preferred orientation according to E_{int}, i.e., *(1 0 1)* < *(1 0 0)* < *(0 0 1)* < *(1 1 0)*, is similar for both T and O surfaces, only in the case of edge *(0 0 1)* ≈ *(1 1 0)*. T surface is strongly preferred by *(1 0 1)* and *(1 0 0)* planes of ZnO NP, while *(0 0 1)* plane does not distinguish between T and O surface. Orientation of ZnO NP via *(1 1 0)* plane slightly prefers the edge. The strongest interaction (i.e., the best mutual compatibility) between T surface and *(1 0 1)* plane shows the most preferred orientation of ZnO NPs. In the case of monocrystalline NPs, the adjacent plane is the same as the top plane accessible to the AO7 molecules. Strong photocatalytic activity of the *(1 0 1)* plane [15] suggests good photocatalytic properties of nanocomposite containing such preferentially oriented ZnO NPs.

Photocatalytic activities of the samples are shown in **Figure 3**. Dried samples exhibit similar and very low photocatalytic activity; ~ 3 mg of AO7 per 1 g of the photocatalyst was degraded. Calcination at 400 °C led to increase in photocatalytic activity which is again similar for both types of samples but nearly ten times higher than in the previous case. Further increase in calcination temperature had a different effect for each type of

samples. While in the case of pure NPs the photocatalytic activity increased up to 600 °C when the value ~ 53 mg·g^{-1} was reached, the nanocomposites exhibits similar photocatalytic activity ~ 40 mg·g^{-1} both for 500 and 600 °C. Taking into account that K-ZnO nanocomposite contains only 38.7 wt.% of ZnO (**Table 1**), the photoactivity of the nanocomposite calcined at 600 °C is in fact two times higher than the photoactivity of the pure ZnO NPs. This can be explained by smaller size of ZnO NPs in the nanocomposite and mainly by their uniform distribution on the surface of kaolin (**Figure 2**) resulting in a larger surface of ZnO accessible to AO7 molecules.

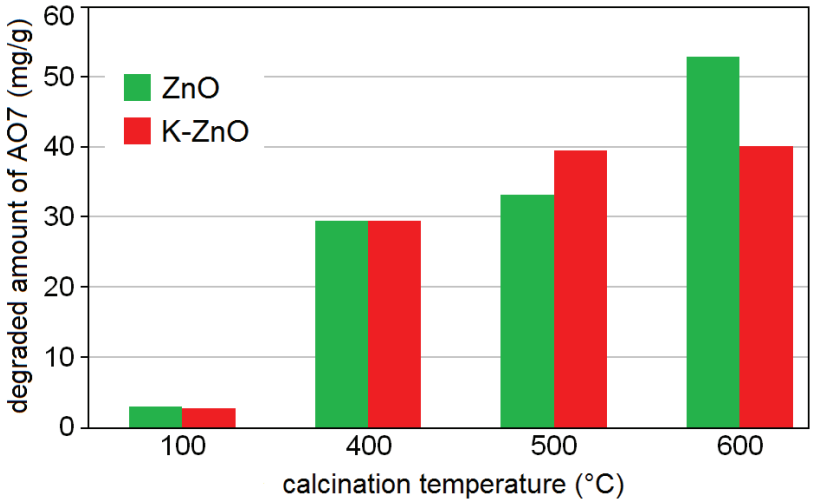

Figure 3 Degraded amounts of AO7 for ZnO NPs and K-ZnO nanocomposites dried at 100 °C and calcined at 400 - 600 °C

Leaching tests performed on the calcined composites revealed that 0.13, 0.15, and 0.20 mg of Zn per 1 dm^3 of water was released from K-ZnO(400), K-ZnO(500), and K-ZnO(600), respectively. This amount is much lower than the maximum permissible limit of Zn in drinking water for Czech Republic (3.0 mg·dm^{-3} [16]), and also lower than 1.2 mg·dm^{-3}, i.e., the limit for leachates of materials than can be considered as inert in the European Union [17]. Important finding is also negligible decrease (~ 1 %) in photocatalytic activity of the K-ZnO nanocomposites after the leaching tests. This fact together with low amount of Zn released during leaching is evidence of stability of the nanocomposites.

4. CONCLUSION

K-ZnO nanocomposite prepared by calcination process from sodium zinc carbonate clusters formed on the surface of kaolin particles is promising photocatalytic material. Containing ~ 39 wt.% of ZnO NPs, the nanocomposite calcined at 500 or 600 °C exhibits the photoactivity against AO7 two times higher in comparison with pure ZnO NPs calcined at 600 °C. Strong anchoring of the ZnO NPs on the kaolin was proved by leaching test that showed the nanocomposite to be environmentally safe. Tests of photocatalytic activity of the nanocomposite performed after the leaching showed no significant difference in comparison with the tests performed before leaching, i.e., stability of the nanocomposite was confirmed. Photocatalytic properties of ZnO NPs in nanocomposite are not affected by anchoring on kaolin. Band gap energy of ZnO NPs in nanocomposite is similar to band gap energy of pure ZnO NPs. The fact that calcination at 500 °C is sufficient to achieve photocatalytic activity two times higher in comparison with pure ZnO NPs calcined at 600 °C is economic benefit of the nanocomposite. However, taking into account the kaolinite → metakolinite phase transformation at 600 °C, calcination at temperature higher than 500 °C also brings advantage due to pozzolanic activity of the metakaolinite. Therefore, the nanocomposite can find its use in building industry, e.g. as a functional component of plasters.

ACKNOWLEDGEMENTS

This research has been funded by the Ministry of Education, Youth and Sports of the Czech Republic (projects numbers SP2016/63, SP2017/65, LQ1602 (National Programme of Sustainability II - IT4Innovations excellence in science).

REFERENCES

[1] MISAO, Y., ZHANG, H., YUAN, S., JIAO, Z., ZHU, X. Preparation of flower-like ZnO architectures assembled with nanosheets for enhanced photocatalytic activity. Journal of Colloid and Interface Science, 2016, vol. 462, pp. 9-18.

[2] FATIMAH, I., WANG, S., WULANDARI, D. ZnO/montmorillonite for photocatalytic and photochemical degradation of methylene blue. *Applied Clay Science*, 2011, vol. 53, no. 4, pp. 553-560.

[3] HAYAT, K., GONDAL, M. A., KHALED, M. M., AHMED, S., SHEMSI, A. M. Nano ZnO synthesis by modified sol gel method and its application in heterogeneous photocatalytic removal of phenol from water. *Applied Catalysis A*, 2011, vol. 393, pp. 122-129.

[4] SRIVASTAVA, V., GUSAIN, D., SHARMA, Y. C. Synthesis, characterization and application of zinc oxide nanoparticles (n-ZnO). *Ceramics International*, 2013, vol. 39, no. 8, pp. 9803-9808.

[5] TOBÓN-ZAPATA, G. E., ETCHEVERRY, S. B., BARAN, E. J. $Na_2Zn_3(CO_3)_4 \cdot 3H_2O$: A potentionally useful compound for zinc supplementation. *Journal of Trace Elements in Medicine and Biology*, 1998, vol. 12, no. 4, pp. 236-239.

[6] YOO, J. D., VOLOVITCH, P. The effect of synthetic zinc corrosion products on corrosion of electrogalvanized steel. I. Catodic reactivity under zinc corrosion products. *Corrosion Science*, 2014, vol. 81, pp. 11-20.

[7] SEKER, S., ELÇIN, A. E., YUMAK, T., SINAG, A., ELÇIN, Y. M. In vitro cytotoxicity of hydrothermally synthesized ZnO nanoparticles on human periodontal ligament fibroblast and mouse dermal fibroblast cells. *Toxicology in Vitro*, 2014, vol. 28, no. 8, pp. 1349-1358.

[8] BACCHETTA, R., MOSCHINI, E., SANTO, N., FASCIO, U., DEL GIACCO, L., FREDDI, S., CAMATINI, M., MANTECCA, P. Evidence and uptake routes for zinc oxide nanoparticles through the gastrointestinal barrier in Xenopus laevis. *Nanotoxicology*, 2014, vol. 8, no. 7, pp. 728-744.

[9] MATĚJKA, V., TOKARSKÝ, J. Photocatalytical nanocomposites: A review. *Journal of Nanoscience and Nanotechnology*, 2014, vol. 14, no. 2, pp. 1597-1616.

[10] MAMULOVÁ KUTLÁKOVÁ, K., TOKARSKÝ, J., PEIKERTOVÁ, P. Functional and eco-friendly nanocomposite kaolinite/ZnO with high photocatalytic activity. *Applied Catalysis B*, 2015, vol. 162, pp. 392-400.

[11] SHVARZMAN, A., KOVLER, K., GRADER, G. S., SHTER, G. E. The effect of dehydroxylation/amorphization degree on pozzolanic activity of kaolinite. *Cement and Concrete Research*, 2003, vol. 33, no. 3, pp. 405-416.

[12] MATĚJKA, V., MATĚJKOVÁ, P., KOVÁŘ, P., VLČEK, J., PŘIKRYL, J., ČERVENKA, P., LACNÝ, Z., KUKUTSCHOVÁ, J. Metakaolinite/TiO_2 composite: Photoactive admixture for building materials based on Portland cement binder. *Construction and Building Materials*, 2012, vol. 35, pp. 38-44.

[13] RAPPE, A. K.. CASEWIT, C. J., COLWELL, K. S., GODDARD, W. A., SKIFF, W. M. UFF, a full periodic table force field for molecular mechanics and molecular dynamics simulations. *Journal of the American Chemical Society*, 1992, vol. 114, no. 25, pp. 10024-10035.

[14] SCHERRER, P. Estimation of size and internal structure of colloidal particles by means of Röntgen rays. *Nachrichten von der Gesellschaft der Wissenschaften zu Gottingen*, 1918, vol. 2, pp. 96-100.

[15] ZHOU, X., XIE, Z. X., JIANG, Z. Y., KUANG, Q., ZHANG, S. H., XU, T., HUANG, R. B., ZHENG, L. S. Formation of ZnO hexagonal micro-pyramids: a successful control of the exposed polar surfaces with the assistance of an ionic liquid. Chemical Communications, 2005, vol. 44, pp. 5572-5574.

[16] CZECH MINISTRY OF HEALTH. Announcement of Czech Ministry of Health No.252/2004 Coll, 2004. *Collection of Laws of the Czech Republic*. 82. pp. 5402-5422.

[17] COUNCIL OF THE EUROPEAN UNION. Council decision of 19 December 2002 establishing criteria and procedures for the acceptance of waste at landfills pursuant to Article 16 of and Annex II to Directive 1999/31/EC (2003/33/EC). *Official Journal of the European Communities*, 2003, vol. 46, pp. L11/27-L11/49.